



LETTER TO THE EDITOR

H3K14me3 genomic distributions and its regulation by KDM4 family demethylases

Cell Research (2018) 28:1118–1120;
<https://doi.org/10.1038/s41422-018-0095-6>

Dear Editor,

Histone lysine methylations are essential components of the epigenetic regulatory mechanisms. Although major histone lysine methylations have been extensively investigated, low-abundance methylations remain largely elusive. Among the low-abundance methylations, H3K14me3 has been identified in mammalian cells upon pathological infection by *Legionella pneumophila*, a gram-negative bacterium and causative agent of a severe form of pneumonia. Global host chromatin H3K14 trimethylation and transcription repression are mediated by an H3K14 methyltransferase, regulator of methylation A (RomA) encoded by the bacterial genome.¹ Importantly, previous mass spectrometry studies also suggested the presence of endogenous H3K14 methylations among eukaryotes,^{2–7} although these findings have not been confirmed by independent means. In addition, the genomic distribution as well as the H3K14me3 regulatory enzymes have not been identified. Here, using an H3K14me3-specific antiserum we report the identification of distinct and shared H3K14me3 distribution patterns in HEK293T and human embryonic stem cells (hESCs), two cell lines with extensive epigenome profiles allowing cross comparisons with other known histone marks. H3K14me3 heavily decorates the KRAB-ZNF (Krupple-associated box containing zinc finger gene) clusters in both HEK293T and hESC cells but is only strongly associated with active transcription in HEK293T cells, where it binds thousands of active promoters. We further profiled H3K14me3 in a mouse melanoma cell line, B16, and discovered similar distribution features to those in HEK293T cells. Importantly, we identified members of the KDM4 family of histone demethylases (KDM4A, KDM4B and KDM4C) as H3K14me3 demethylases. As the KDM4 family members have been shown to mediate H3K9me3 and H3K36me3 demethylation,⁸ our findings also revealed crosstalks among these modifications.

To understand H3K14me3 regulation and function, we first set out to confirm the previous mass spectrometry results by generating a highly specific antiserum for H3K14me3. We used a branched peptide (H3 11–20 aa) as antigen, and the resulting antiserum demonstrated substrate specificity towards H3K14me3 in various specificity tests (Supplementary information, Fig. S1a–e). Using the antiserum, we detected H3K14me3 signals in protein extracts from human and mouse cell lines, and in calf thymus histones (Supplementary information, Fig. S1f), and its abundance in HEK293T cells was estimated to be ~0.4% of total histone H3 protein (Supplementary information, Fig. S1g), consistent with a recent study.² We then used the antiserum to profile H3K14me3 genomic distributions in both HEK293T and hESC cells. In HEK293T cells, we identified 10,393 H3K14me3 peaks, and notably, these binding events were enriched > 5-fold at the Transcription Start Site (TSS) regions (13.3% vs. 2.3% of genome average), and moderately enriched over exonic regions

(8.1% vs. 3.2% of genome average) (Fig. 1a). Through systematic comparisons with other well-studied histone H3 trimethylations, we found that H3K14me3 co-existed with H3K4me3 at 1,387 TSS regions, and also identified an association, albeit weak, with H3K9me3 over the non-TSS regions (Fig. 1b). In contrast, H3K14me3 and H3K27me3 appeared to be mutually exclusive (Fig. 1b). Importantly, H3K14me3 was strongly associated with active transcription (Fig. 1c), and the transcription levels of genes decorated by H3K14me3 were significantly higher than the genome average in HEK293T cells (Supplementary information, Fig. S2a).

In hESCs, we identified significantly more H3K14me3 peak regions (22,126), and most of them fell into intergenic regions (Fig. 1a). The relative intensities of H3K14me3 peaks in hESCs were much lower compared to the peaks in HEK293T cells, although its enrichments over KRAB-ZNF genes were comparable between the two cell lines (Fig. 1d and see below). Further analyses only identified a modest association of H3K14me3 with H3K9me3 and H3K36me3 in hESCs (Supplementary information, Fig. S2b), a pattern very different from that in HEK293T cells. Notably, instead of enrichment over TSS regions found in HEK293T, H3K14me3 was generally depleted at TSSs in hESCs (Fig. 1d; Supplementary information, Fig. S2c). Consistently, we also failed to observe a clear correlation of H3K14me3 with active transcription in hESCs (Supplementary information, Fig. S2c), indicating potentially differential regulation and functions of H3K14me3 in the two cell lines.

We next analyzed H3K14me3-decorated genes in both cell lines, and identified 6,487 and 3,022 target genes in HEK293T and hESC cells (Supplementary information, Fig. S3a), respectively. Interestingly, ZNF (Zinc-Finger containing) genes, especially KRAB-ZNF genes, represent the top functional category of H3K14me3-decorated genes in both cell lines (Supplementary information, Fig. S3b). Consistently, among the 1,217 shared target genes in both cell lines, 383 are ZNF genes (Supplementary information, Fig. S3c, significantly enriched). Significantly, H3K14me3 enrichments over KRAB-ZNF gene clusters were also much higher than other genes (Fig. 1d), which was readily observable even at the layer of chromosomal view of Chromosome 19 (Supplementary information, Fig. S3d–e). Of note, chromosome 19 contains most H3K14me3 target genes since it possesses most KRAB-ZNF gene clusters in human genome.

To further extend our understanding of H3K14me3, we performed H3K14me3 ChIP-seq analyses in a mouse melanoma cell line, B16 (Supplementary information, Fig. S4a). Our ChIP-seq identified 10,659 H3K14me3 peaks covering 9,325 genes in the B16 genome. Interestingly, we found that H3K14me3 in B16 cells showed similar distribution features to those in HEK293T cells, including a significant enrichment at promoter regions (23.5% versus 1.1% as control), positive correlations with transcription, as well as stronger enrichment over ZNF gene bodies compared to

Received: 12 May 2018 Revised: 20 August 2018 Accepted: 4 September 2018
Published online: 18 October 2018

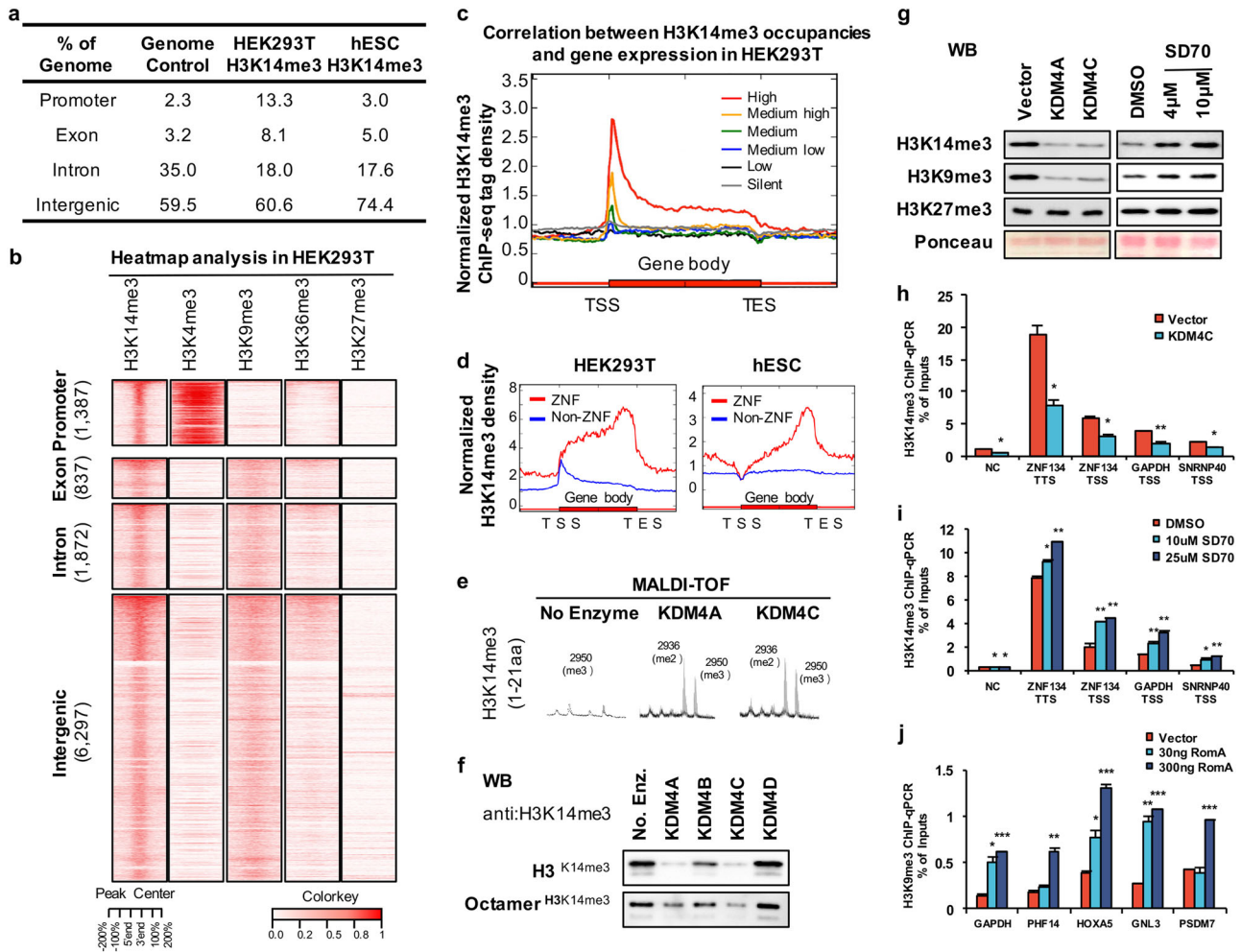


Fig. 1 **a** Genomic distribution of H3K14me3 ChIP-seq peaks in HEK293T and hESC cells. **b** Heatmap analysis of the co-occupancy of H3K14me3 and other major histone lysine trimethylations in HEK293T cells. **c** H3K14me3 ChIP-seq densities are profiled according to the indicated expression levels of the target genes in HEK293T cells. **d** Distribution of H3K14me3 over the gene bodies of the ZNF and non-ZNF target genes in HEK293T (left) and hESC (right) cells. **e** MALDI-TOF analyses of KDM4A and 4C activities on H3K14me3 peptides. **f** Western blot analyses of KDM4 demethylase activities on the histone H3 and octamer premethylated by RomA. **g** Western blot analyses of the indicated histone methylation levels in KDM4A- and KDM4C-overexpressing or SD70-treated HEK293T cells. **h, i** ChIP-qPCR analyses of H3K14me3 levels at the selected loci in HEK293T cells with KDM4C overexpression (**h**) and SD70 treatment (**i**). TSS: transcription start site, TTS: transcription termination site, NC: negative control. **j** ChIP-qPCR analyses of H3K9me3 levels at the selected active gene promoters in RomA-overexpressing HEK293T cells. All q-PCR data are represented as mean \pm SD from two biological replicates. * $P < 0.05$; ** $P < 0.01$; *** $P < 0.001$, T test

Non-ZNF genes (Supplementary information, Fig. S4b-d). These findings suggest that H3K14me3 may be subjected to similar regulations in B16 and HEK293T cells.

We next wished to identify methyltransferases and demethylases of H3K14me3 using a candidate approach (Supplementary information, Fig. S5a). This approach led to the identification of KDM4A, 4B and 4C, which robustly demethylated H3K14me3 to H3K14me2 on peptide substrates (Fig. 1e; Supplementary information, Fig. S5b). Interestingly, the closely related family member, KDM4D, showed no activity under the same assay conditions (Supplementary information, Fig. S5b). Of note, when demethylating H3K9me3 and H3K36me3, KDM4 enzymes are capable of removing one or two methyl groups, resulting in di- and mono-methylated products⁸ (Supplementary information, Fig. S5b, right). However, these enzymes could only remove a single methyl group from H3K14me3 to yield di-methylated products in vitro (Supplementary information, Fig. S5b, left). Consistently, these enzymes also showed no activities towards H3K14me2 peptides (Supplementary information, Fig. S5b, middle). To further characterize the robustness of H3K14me3

demethylation mediated by the KDM4 enzymes, we compared KDM4C activities towards H3K14me3 and H3K9me3 peptides. As shown in Supplementary information, Fig. S5c, KDM4C showed comparable activities towards H3K14me3 and H3K9me3 peptides ($K_{cat}[H3K14me3] = 0.019 s^{-1}$, $K_{cat}[H3K9me3] = 0.064 s^{-1}$). Consistently, the substrate K_m s were also comparable ($K_m[H3K14me3] = 1.65 \mu M$ and $K_m[H3K9me3] = 1.03 \mu M$; Supplementary information, Fig. S5c). We next utilized RomA to generate H3K14me3-decorated recombinant histone H3 and octamers, and found that KDM4A/4B/4C were also active in removing H3K14me3 from these substrates (Fig. 1f). Again, we found that KDM4A and 4C showed stronger activities than KDM4B, whereas KDM4D showed no activity (Fig. 1f). These data further demonstrated that KDM4A, 4B and 4C are H3K14me3 demethylases in vitro.

To further explore whether KDM4 enzymes regulate H3K14me3 in cells, we took advantage of the previous findings that overexpression of KDMs generally resulted in detectable, global demethylation in cultured cells.⁸ In support of our in vitro findings, KDM4A and 4C overexpression significantly reduced the global level of H3K14me3 in HEK293T cells (Fig. 1g, left). In addition, we

confirmed reduction of H3K14me3 at 4 out of 4 selected genomic regions (identified by ChIP-seq assays) (Fig. 1h). Consistently, treating cells with a reported KDM4C inhibitor, SD70,⁹ led to a significant increase of both the global and site-specific levels of H3K14me3 (Fig. 1g, right, and Fig. 1i).

Finally, we found that RomA, encoded by *Legionella pneumophila* genome, could induce a significantly higher level of ectopic H3K14me3 when compared to the endogenous H3K14me3 level as reported¹ (Supplementary information, Figs. S5d and S1d-e). We thus hypothesize that such ectopic H3K14me3 sites could compete for the KDM4 enzymes and therefore reduce available enzymes for demethylating H3K9me3 and H3K36me3. Supporting our hypothesis, RomA overexpression indeed led to a significant, albeit moderate, increase of H3K9me3 and H3K36me3 levels (Supplementary information, Fig. S5d). Importantly, we also observed an apparent increase of H3K9me3 along with H3K14me3 at 5 randomly selected active promoter regions, where were absent of H3K9me3 in the control HEK293T cells, upon ectopic expression of RomA (Fig. 1j).

In summary, we identified distinct genomic distributions of endogenous H3K14me3 in human and mouse cells (HEK293T, hESC and mouse B16 cells), and uncovered a strong association of this modification with active transcription in HEK293T and B16 melanoma cells. In contrast, we did not observe an association of H3K14me3 with active transcription in hESCs, suggesting a differential regulation in hESCs. We also found that KRAB-ZNF genes are enriched for high levels of H3K14me3 over the gene bodies in all three cell lines and represent the top functional group of H3K14me3-decorated genes shared by HEK293T and hESC cells. Importantly, we identified KDM4A, 4B and 4C as demethylases for H3K14me3 both in vitro and in vivo, and revealed a previously unappreciated crosstalk between H3K14me3 and H3K9me3/H3K36me3.

Of note, our data demonstrate that KDM4 family demethylases are only able to catalyze H3K14me3 to H3K14me2, suggesting that H3K14me2 may, as another potential histone mark, play roles in epigenetic regulation and its demethylation to mono- and unmethylated forms may involve different mechanisms. With recent mass spectrometry studies detecting all three methyl forms of H3K14 in a mouse epithelial to mesenchymal cell culture model,² we believe that investigations in the future will shed further light on the roles and regulations of H3K14 methylations.

Histone H3K14 residue could also be acetylated, which is associated with gene activation. The abundance of H3K14Ac has been measured to be ~20%-30% in human cell lines.² Our data estimated the abundance of H3K14me3 to be ~0.4% in HEK293T cells (Supplementary information, Fig. S1g), indicating a locus-specific function. It is conceivable that a single histone H3 tail can either be methylated or acetylated, thus H3K14me3 could potentially be involved in gene regulation by antagonizing H3K14Ac. Importantly, RomA orthologs have been found in several *Legionella* strains causing lung infection in humans and animals, and it has been reported as a transcriptional repressor by suppressing H3K14Ac through its robust activity towards H3K14me3.¹ Our observation now raises another interesting possibility that RomA may compromise H3K9me3 and H3K36me3 similarly during infection.^{1,10} Since our analyses were carried out in an overexpression system, this hypothesis will have to be tested experimentally in an infection model in the future.

ACKNOWLEDGEMENTS

We thank Dr. Ning Sun (Fudan University) for H7 human ES cell lines and Drs. Bing Zhu and Guohong Li (IBP-CAS) for technical assistance with MLA

histones and nucleosome assembly. Fei Lan was funded by State Key development program (MOST) (2016YFA0101800), the National Natural Science Foundation of China (31371303), Shanghai Municipal Education Commission (SHMEC) (14ZZ006) and Shanghai Municipal Science and Technology Major Project (2017SHZDZX01).


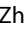
AUTHOR CONTRIBUTIONS

B.Z. and F.L. initiated the project and developed the main concept of the study with the help from Y.S. B.Z., B.R., X.Y., R.D. carried out all of the experiments. W.X., G.C., W.L. completed all bioinformatics analyses under the guidance from J.H. and F.L., J. Chen and R.Z. provided mass spec support. J. Cai, L. S. and Z.-Q.L. provided necessary materials for revision. B.Z., Y.S. and F.L. wrote the manuscript together.

ADDITIONAL INFORMATION

Supplementary information accompanies this paper at <https://doi.org/10.1038/s41422-018-0095-6>.

Competing interests: The authors declare no competing interests.

Bin Zhao¹ , Wenqi Xu¹, Bowen Rong¹, Guoyu Chen², Xuanjia Ye¹, Ruofei Dai¹, Wenjing Li¹, Jiajia Chen³, Jiajun Cai⁴, Lei Song⁵, Zhao-Qing Luo⁵ , Rong Zeng⁶, Yang Shi⁷, Jing-Dong J. Han² and Fei Lan¹

¹Liver Cancer Institute, Zhongshan Hospital, Fudan University, Key Laboratory of Carcinogenesis and Cancer Invasion, Ministry of Education, Key Laboratory of Epigenetics and Metabolism, Ministry of Science and Technology, and Institutes of Biomedical Sciences, Fudan University, Shanghai 200032, China; ²Key Laboratory of Computational Biology, CAS Center for Excellence in Molecular Cell Science, Collaborative Innovation Center for Genetics and Developmental Biology, Chinese Academy of Sciences-Max Planck Partner Institute for Computational Biology, Shanghai Institutes for Biological Sciences, Chinese Academy of Sciences, 320 Yue Yang Road, Shanghai 200031, China; ³Institutes of Biomedical Sciences and Department of Systems Biology for Medicine, Basic Medical College, Fudan University, Shanghai 20032, China; ⁴Department of Neurosurgery Huashan Hospital, Fudan University, Shanghai 200040, China; ⁵Department of Respiratory Medicine, Center of Infection and Immunity, The First Hospital, Jilin University, Changchun, Jilin 130001, China; ⁶Key Laboratory of Systems Biology, Institute of Biochemistry and Cell Biology, Shanghai Institutes for Biological Science, Chinese Academy of Sciences, Shanghai 200031, China and ⁷Newborn Medicine Division, Boston Children's Hospital and Department of Cell Biology, Harvard Medical School, Boston, MA 02115, USA

These authors contributed equally: Wenqi Xu, Bowen Rong and Guoyu Chen

Correspondence: Fei Lan (fei_lan@fudan.edu.cn)

REFERENCES

1. Rolando, M. et al. *Cell Host Microbe* **13**, 395–405 (2013).
2. Sidoli, S. et al. *Epigenet. Chromatin* **10**, 34 (2017).
3. Bonenfant, D. et al. *Mol. Cell. Proteom.* **6**, 1917–32 (2007).
4. Tweedie-Cullen, R. Y. et al. *PLoS One* **7**, e36980 (2012).
5. Jung, H. R., Pasini, D., Helin, K. & Jensen, O. N. *Mol. Cell. Proteom.* **9**, 838–50 (2010).
6. Garcia, B. A. et al. *J. Biol. Chem.* **282**, 7641–55 (2007).
7. McKittrick, E., Gaften, P. R., Ahmad, K. & Henikoff, S. *Proc. Natl Acad. Sci. USA* **101**, 1525–30 (2004).
8. Whetstine, J. R. et al. *Cell* **125**, 467–81 (2006).
9. Jin, C. et al. *Proc. Natl Acad. Sci. USA* **111**, 9235–40 (2014).
10. Michard, C. & Doublet, P. *Front. Microbiol.* **6**, 87 (2015).